

COARSE-GRAINED ENTROPY RATES QUANTIFY FAST Ca^{2+} DYNAMICS MODULATED BY PHARMACOLOGICAL STIMULATION

M. PALUŠ

*Institute of Computer Science, Academy of Sciences of the Czech Republic,
Pod vodárenskou věží 2, 182 07 Prague 8, Czech Republic*

C. SCHÖFL, A. VON ZUR MÜHLEN, G. BRABANT, K. PRANK
*Department of Clinical Endocrinology, Medical School Hannover,
Carl-Neuberg-Str. 1, D-30625 Hannover, Germany*

Calcium (Ca^{2+}) is an ubiquitous intracellular messenger which regulates cellular processes, such as secretion, contraction, and cell proliferation^{1,2}. A variety of cell types respond to hormonal stimuli with periodic oscillations of the intracellular free Ca^{2+} concentration ($[\text{Ca}^{2+}]_i$) which can be modulated in their frequency in a dose-dependent manner. The period of these well-studied oscillations varies normally between 30 sec and a couple of minutes. Here we study $[\text{Ca}^{2+}]_i$ oscillations in clonal β cells (hamster insulin secreting cells, HIT) under pharmacological stimulation. Besides the well-known high-amplitude low frequency oscillations we try to analyze for the first time low-amplitude high frequency oscillations of $[\text{Ca}^{2+}]_i$ under pharmacological stimulation which have not been explored in experimental approaches to date. Using coarse-grained entropy rates computed from information-theoretic functionals we demonstrate differences in temporal complexity of the fast low-amplitude $[\text{Ca}^{2+}]_i$ dynamics corresponding to different phases of pharmacological stimulation which are additional to the well-known dose-dependent pattern of low-frequency high amplitude $[\text{Ca}^{2+}]_i$ dynamics.

1 Introduction

Consider a complex, dynamic process evolving in time. A series of measurements done on such a system in consecutive instants of time $t = 1, 2, \dots$ is usually called a time series $\{y(t)\}$. Consider further that the temporal evolution of the studied system is not completely random, i.e., that the state of the system in time t in some way depends on the state in which the system was in time $t - \tau$. The strength of such a dependence per a unit time delay τ , or, inversely, a rate at which the system “forgets” information about its previous states, can be an important quantitative characterization of temporal complexity in the system’s evolution. The time series $\{y(t)\}$, which is a recording of (a part of) the system temporal evolution, can be considered as a realization of a stochastic process, i.e., a sequence of stochastic variables. Uncertainty in a stochastic variable is measured by its *entropy*. The rate in which the stochastic process “produces” uncertainty is measured by its *entropy rate*. The concept

of entropy rates is common to the theory of stochastic processes as well as to the information theory where the entropy rates are used to characterize information production by information sources³.

Alternatively, the time series $\{y(t)\}$ can be considered as a projection of a trajectory of a dynamical system, evolving in some measurable state space. A. N. Kolmogorov, who introduced the theoretical concept of classification of dynamical systems by information rates⁴, was inspired by the information theory and generalized the notion of the entropy of an information source^{4,5,8}. The Kolmogorov-Sinai entropy (KSE)^{5,6,7,8} is a topological invariant, suitable for classification of dynamical systems or their states, and is related to the sum of the system's positive Lyapunov exponents (LE) according to the theorem of Pesin⁹.

Thus, the concept of entropy rates is common to theories based on philosophically opposite assumptions (randomness vs. determinism) and is ideally applicable for characterization of complex biological processes, where possible deterministic rules are always accompanied by random influences.

In this paper we demonstrate an application of so-called coarse-grained entropy rates for the characterization and segmentation of high-frequency oscillations of intracellular Ca^{2+} ($[\text{Ca}^{2+}]_i$) in clonal β cells (insulin secreting hamster cells) induced by a hormonal agonist (arginin-vasopressin, AVP) and synergistically activated by increasing doses of an additional agonist (tolbutamide).

2 Information-Theoretic Functionals and Entropy Rates

Consider n discrete random variables X_1, \dots, X_n with sets of values Ξ_1, \dots, Ξ_n , respectively. The probability distribution for an individual X_i is $p(x_i) = \Pr\{X_i = x_i\}$, $x_i \in \Xi_i$. We denote the probability distribution function by $p(x_i)$, rather than $p_{X_i}(x_i)$, for convenience. Analogously, the joint distribution for the n variables X_1, \dots, X_n is $p(x_1, \dots, x_n) = \Pr\{(X_1, \dots, X_n) = (x_1, \dots, x_n)\}$, $(x_1, \dots, x_n) \in \Xi_1 \times \dots \times \Xi_n$.

The marginal redundancy $\varrho(X_1, \dots, X_{n-1}; X_n)$, in the case of two variables also known as mutual information $I(X_1; X_2)$, quantifies the average amount of information about the variable X_n , contained in the $n - 1$ variables X_1, \dots, X_{n-1} , and is defined as

$$\varrho(X_1, \dots, X_{n-1}; X_n) = \sum_{x_1 \in \Xi_1} \dots \sum_{x_n \in \Xi_n} p(x_1, \dots, x_n) \log \frac{p(x_1, \dots, x_n)}{p(x_1, \dots, x_{n-1})p(x_n)}. \quad (1)$$

Now, let $\{X_i\}$ be a stochastic process, i.e., an indexed sequence of random variables, characterized by the joint probability distribution function $p(x_1, \dots, x_n)$. The entropy rate of $\{X_i\}$ is defined as

$$h = \lim_{n \rightarrow \infty} \frac{1}{n} H(X_1, \dots, X_n), \quad (2)$$

where $H(X_1, \dots, X_n)$ is the joint entropy of the n variables X_1, \dots, X_n with the joint distribution $p(x_1, \dots, x_n)$:

$$H(X_1, \dots, X_n) = - \sum_{x_1 \in \Xi_1} \dots \sum_{x_n \in \Xi_n} p(x_1, \dots, x_n) \log p(x_1, \dots, x_n). \quad (3)$$

A way from the entropy rate of a stochastic process to the Kolmogorov-Sinai entropy (KSE) of a dynamical system can be straightforward due to the fact that any stationary stochastic process correspond to a measure-preserving dynamical system, and vice versa⁷. Then for the definition^a of the KSE we can consider the equation (2), however, the variables X_i should be understood as m -dimensional variables, according to a dimensionality of the dynamical system. If the dynamical system is evolving in continuous (probability) measure space, then any entropy depends on a partition ξ chosen to discretize the space and the KSE is defined as a supremum over all finite partitions^{6,7,8}.

Possibilities to compute the entropy rates from data are limited to a few exceptional cases: for stochastic processes it is possible, e.g., for finite-state Markov chains³. In the case of a dynamical system on continuous measure space, the KSE can be, in principle, reliably estimated if the system is low-dimensional and a large amount of (practically noise-free) data is available. In such a case, Fraser¹⁰ proposed to estimate the KSE of a dynamical system from the asymptotic behavior of the marginal redundancy, computed from a time series generated by the dynamical system. In such an application one deals with a time series $\{y(t)\}$, considered as a realization of a stationary and ergodic stochastic process $\{Y(t)\}$. Then, due to ergodicity, the marginal redundancy (1) can be estimated using time averages instead of ensemble averages, and, the variables X_i are substituted as

$$X_i = y(t + (i - 1)\tau). \quad (4)$$

Due to stationarity the marginal redundancy

$$\varrho^n(\tau) \equiv \varrho(y(t), y(t + \tau), \dots, y(t + (n - 2)\tau); y(t + (n - 1)\tau)) \quad (5)$$

^aA more detailed and rigorous KSE definition can be found in monographs^{6,7,8} or in the paper of Paluš¹² and references therein.

is a function of n and τ , independent of t .

It was shown^{10,11,12} that if the underlying dynamical system is m -dimensional and the marginal redundancy $\varrho^n(\tau)$ is estimated using a partition fine enough (to attain so-called generating partition^{6,8,10}), then the asymptotic behavior

$$\varrho^n(\tau) \approx H_1 - |\tau|h \tag{6}$$

is attained for $n = m + 1, m + 2, \dots$, for some range of τ . The constant H_1 is related to $\varrho^n(0)$.

3 Coarse-Grained Entropy Rates

The equation (6) gives the relation between the asymptotic behaviour of the information-theoretic functional – the marginal redundancy $\varrho^n(\tau)$ estimated from a time series, and the KSE of a dynamic system underlying the time series. It was demonstrated^{12,13} that for observation of the behaviour (6), a large amount of data is necessary, which make possible to estimate a probability distribution on a generating partition. In experimental practice, however, the analyzed time series are usually short and contaminated by noise, so even if they resulted from low-dimensional chaotic processes, estimation of their KSE is practically impossible^{12,13}. And in many experiments, actual dynamical mechanisms, underlying analyzed data, are unknown, and can be either high-dimensional deterministic or stochastic. As we have pointed above, unlike other dynamical characteristics (such as dimensions or Lyapunov exponents), the entropy rates are meaningful quantities for characterization of stationary processes irrespectively of their origin. The problem is, however, that the exact entropy rate of a process usually cannot be estimated from experimental data. In order to utilize the concept of the entropy rates in time-series analysis, Paluš¹³ has proposed to give up the effort for estimating the exact entropy rates, and to define “coarse-grained entropy rates” (CER’s) instead. The CER’s are not meant as estimates of the exact entropy rates, but as quantities which can depend on a particular experimental and numerical set-up, however, quantities which have the same meaning as the exact entropy rates, i.e., which can be used as measures of regularity and predictability of analyzed time series in the relative sense: Two or several datasets can be compared according to their regularity and predictability, providing they were measured in the same experimental conditions and their CER’s were estimated using the same numerical parameters.

The most straightforward definition¹³ of a CER can be based on (6):

$$h^{(0)} = \frac{\varrho^n(\tau_0) - \varrho^n(\tau_1)}{\tau_1 - \tau_0}. \quad (7)$$

Another type of a CER, providing equivalent characterization of systems, but which might have better numerical properties, Paluš¹³ defines as follows: In a particular application, we compute the marginal redundancies $\varrho^n(\tau)$ for all analyzed datasets and find such τ_{max} that for $\tau' \geq \tau_{max}$: $\varrho^n(\tau') \approx 0$ for all the datasets. Then we define a norm of the marginal redundancy

$$\|\varrho^n\| = \frac{\sum_{\tau=\tau_0}^{\tau_{max}} \varrho^n(\tau)}{\tau_{max} - \tau_0}. \quad (8)$$

Having defined the norm $\|\varrho^n\|$, the difference $\varrho^n(\tau_0) - \|\varrho^n\|$ can be considered as the alternative definition of the CER. It has been found, however, that the definition of the CER, which does not depend on absolute values of $\varrho^n(\tau)$, has better numerical properties, namely the estimates are more stable and less influenced by noise. Thus, we define the CER $h^{(1)}$ as

$$h^{(1)} = \frac{\varrho^n(\tau_0) - \|\varrho^n\|}{\|\varrho^n\|}. \quad (9)$$

The ability of the CER's $h^{(0)}$, $h^{(1)}$ to discern systems with different exact entropy rates, in particular, to discern different states of a chaotic system, is illustrated in Fig. 1. For the well-known chaotic baker map¹⁴, its KSE (or, equivalently, the positive Lyapunov exponent, LE) can be expressed analytically as a function of the system's parameter α (Fig. 1a). Then time series for different values of α were generated and their CER's were computed and plotted as functions of the parameter α (Fig. 1 b-g). Using time series of 16,384 samples, the CER's, especially $h^{(1)}$ provide distinction and classification of the states (with different α) of the baker system equivalently to the analytically computed LE/KSE, i.e., the baker system's exact entropy rate. The numerical stability of the CER estimates decreases with decreasing the length of processed time series (Fig. 1 d-g). Similarly, the CER's discern stochastic processes with different entropy rates¹³.

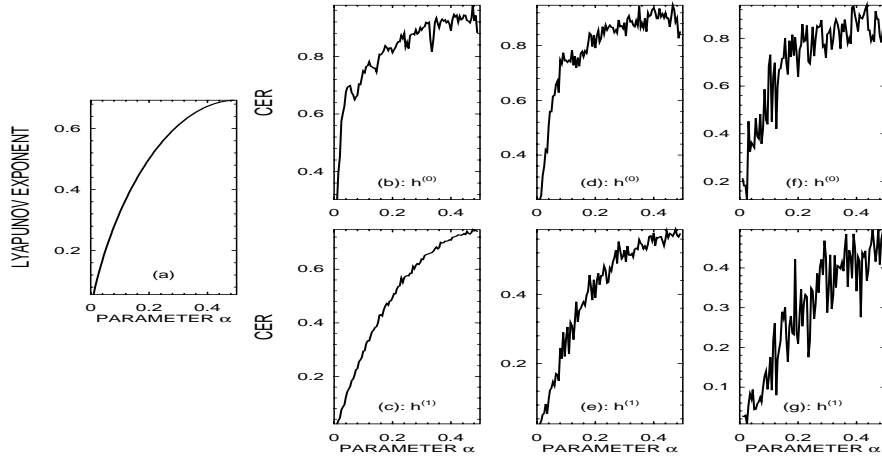


Figure 1: (a) Positive Lyapunov exponent (or Kolmogorov-Sinai entropy) of the chaotic baker map computed as the analytical function of the parameter α . (b–g) Coarse-grained entropy rates $h^{(0)}$ (b,d,f), and $h^{(1)}$ (c,e,g); estimated using the series length $N = 16,384$ (b,c), $N = 1,024$ (d,e), $N = 256$ (f,g), as functions of the parameter α , computed from ninety-seven time series generated by the chaotic baker maps with the parameter α changing from 0.01 to 0.49.

4 Experimental Time Series of $[Ca^{2+}]_i$ in Clonal β - Cells (HIT-Cells)

4.1 Measurements of $[Ca^{2+}]_i$

HIT-T15 cells were kindly provided by W. Knepel (Göttingen, Germany). To measure $[Ca^{2+}]_i$ HIT-cells were subcultured on glass coverslips. The cells were loaded with $5 \mu\text{M}$ Fura-2/AM for 30 min. at 37°C . $[Ca^{2+}]_i$ measurements were done on cells of average size and healthy appearance. Fura-2 fluorescence was recorded from a single cell using a dual excitation spectrofluorometer system (Deltascan 4000, Photon Technology Instruments, Wedel, Germany). All records have been corrected for autofluorescence of unloaded cells at each wavelength before the ratio was used. More details on the measurement of $[Ca^{2+}]_i$ can be found in Schöfl *et al.*¹⁵

4.2 Pharmacological Stimulation

Low-frequency high amplitude $[Ca^{2+}]_i$ oscillations were induced by the administration of 1 nM arginin-vasopressin (AVP). The frequency of the low-frequency high amplitude $[Ca^{2+}]_i$ oscillations was modulated by two different

doses of tolbutamide (3 μM and 10 μM). Through the binding to the sulfonylurea receptor (SUR) tolbutamide inhibits the ATP-sensitive K^+ current ($I_{\text{K}_{\text{ATP}}}$) thereby causing membrane depolarization and activation of Ca^{2+} influx through voltage-dependent calcium channels (VDCC) in β -cells. For the first 500 s only AVP was delivered to the HIT-cell to induce Ca^{2+} oscillations followed by alternating phases of stimulation with tolbutamide and washout phases (see the Legend of Fig. 2 for the exact segments of stimulation). Thus we get $[\text{Ca}^{2+}]_i$ time series with segments of different dynamics depending on the stimulation (Fig. 2).

5 The CER and Ca^{2+} Time Series

The basic idea how to characterize dynamical changes in a time series of Ca^{2+} oscillations is to compute a dynamical characteristic, in this case the CER $h^{(0)}$ (or $h^{(1)}$), in a window moving over the series (i.e., inside overlapping segments of the series). The choice of the window length is usually problematic, since the CER estimated from short series has high variance¹³, while stable estimates from longer windows could either miss a detection of a short-term phenomenon, or could be influenced by possible non-stationarity of the series. In the particular case of the $[\text{Ca}^{2+}]_i$ time series (Fig. 2, the top panel) we analyze five segments of different dynamics, each of them longer than 500 s (500 samples). Therefore, as the first choice we use the window of 512 samples.

The dynamics of the $[\text{Ca}^{2+}]_i$ time series (Fig. 2, the top panel) is clearly dominated by a high-amplitude low-frequency spiky activity, which is evidently different in segments with different doses of tolbutamide stimulation and washout phases respectively. Considering the time scale of the record, however, these Ca^{2+} oscillations are too slow to extract any statistical/information-theoretic characteristic from the available data. A formal application of the CER's estimated in a moving window from the raw $[\text{Ca}^{2+}]_i$ time series (Fig. 2, the top panel) did not lead to distinction of segments of different stimulation. According to our expectation, the low frequency Ca^{2+} spikes cannot be successfully characterized by this approach, and when analyzing Ca^{2+} dynamics on shorter time scales, the spikes can be considered as nonstationarity which effects the analysis and obscures a possible characterization.

Thus our approach focussed on the analysis of the low amplitude high frequency Ca^{2+} oscillations. Let us look at the detailed picture of one of the spikes (Fig. 2, the second panel from the top). Fast oscillations of small amplitudes are apparent on the high-amplitude low frequency spiky dynamics. Therefore we apply a simple high-pass filter realized by subtraction of a three-sample moving average from the raw $[\text{Ca}^{2+}]_i$ time series. The resulting fast

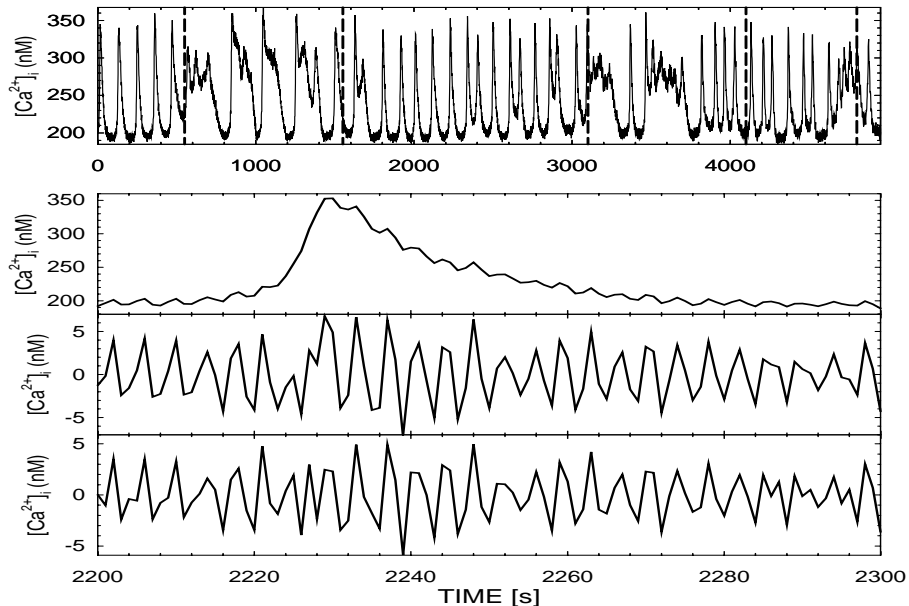


Figure 2: The top panel: Time series of $[Ca^{2+}]_i$ in a single HIT cell sampled at the rate of 1 Hz. Large amplitude Ca^{2+} spikes were induced by the administration of 1 nM argininos-vasopressin (AVP) in segment 1 (0 – 550 s). In the second segment (551 – 1550 s) 10 μM tolbutamide were administered, followed by a washout phase without stimulation (segment 3, 1551 – 3100 s). The tolbutamide dose used in the 4th segment (3101 – 4100 s) was 3 μM . In the 5th segment (4101 – 4800 s) the pharmacological stimulus was removed again. The second panel from the top: Detailed plot of one of the peaks from the $[Ca^{2+}]_i$ time series. The third panel from the top: The same segment of the Ca^{2+} data as in the above panel, but after using a moving-average high-pass filter. The bottom panel: The same segment of the Ca^{2+} data as in the second panel from the top, but after using the moving-average high-pass filter for the second time.

oscillations (Fig. 2, the third panel from the top) still contain some slower phenomena due to the sharp beginning of the Ca^{2+} spike, which can be removed by repeating the same filtering (Fig. 2, the bottom panel, cf. the oscillations around 2230 s in this and in the above panel). The whole $[Ca^{2+}]_i$ time series filtered twice is plotted in the top panel of Figure 3. What is it, this fast dynamics, noisy dynamics without any useful information, or a dynamical, possibly nonlinear process, containing physiologically relevant information? In a preliminary study, a test for nonlinearity¹⁶ applied on different segments of the filtered data yielded statistically significant results (i.e., the null hypothesis of a linear stochastic process has been rejected). Also, it seems that these oscillations possess a property of nonlinear oscillators – a dependence between

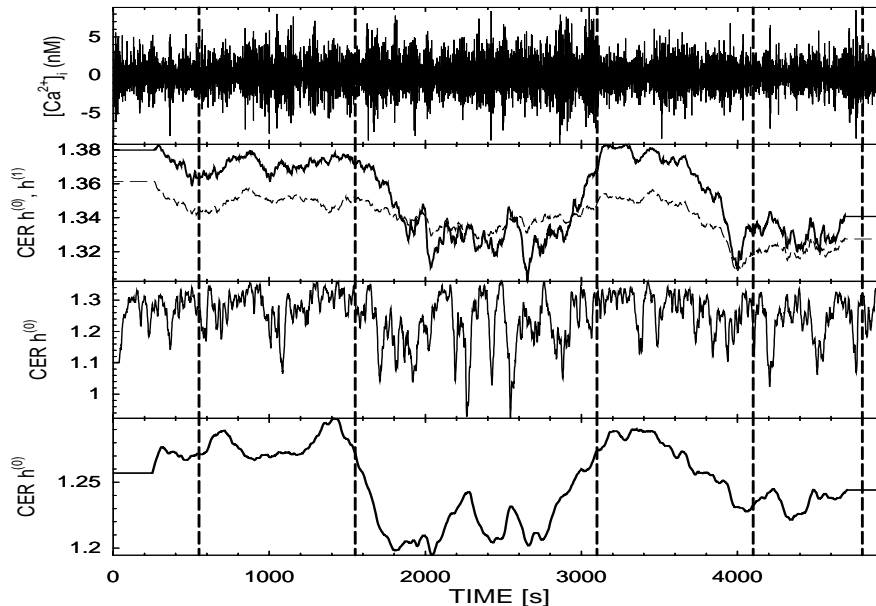


Figure 3: Top panel: The complete $[Ca^{2+}]_i$ time series after twofold moving-average high-pass filtering. The second panel from the top: The CER $h^{(0)}$ (solid line) and $h^{(1)}$ (thin dashed line) estimated in a moving 512-sample window from the above high-pass filtered $[Ca^{2+}]_i$ series. A particular CER value for a window is plotted in the center of that window. The third panel from the top: The CER $h^{(0)}$ estimated in a moving 64-sample window from the above high-pass filtered $[Ca^{2+}]_i$ time series. The bottom panel: The 64-sample window CER (above panel) smoothed by using 511-sample moving average.

instantaneous amplitude and frequency (the waves with lower amplitudes tend to have longer periods). In this paper, however, we focus on the application of the CER's estimated in a moving window as a tool for detecting segments with different temporal complexity. Considering the segments 2 – 5, the CER's (especially $h^{(0)}$), estimated in the 512-sample window (Fig. 3, the second panel from the top) clearly distinguish the segments with (2, 4) and without (3, 5) stimulation.

The CER $h^{(0)}$ computed in the 64-sample window (Fig. 3, the third panel from the top) has a very high variance, which source is numerical, not physiological (cf. Fig. 1 f,g). Smoothed results (Fig. 3, the bottom panel, i.e., the 64-sample window CER has been smoothed by using the 511-sample moving average), however, distinguish the segments with (2, 4) and without stimulation (3, 5) consistently with the results of the above 512-sample window CER.

Considering the question of a statistical significance of the above result,

two different aspects should be distinguished:

a) Are the differences between the CER's, obtained from segments with and without stimulation, statistically significant in general? In other words, is this result a proof that the CER's can distinguish different (stimulation-induced) dynamical modes in the low amplitude high frequency Ca^{2+} oscillations? This question cannot be answered considering the above single time-series measurement. Although a formal application of a statistical test (such as the t-test) on the values of the 512-sample window CER (Fig. 3, the second panel from the top) would yield a significant result, such testing approach would be improper, since the CER values obtained from a moving window cannot be considered as independent measurements. The only way to answer this question is processing a set of independent time series, measured in the same conditions on a set of different cells.

b) Returning back to the above question about the nature of the low amplitude high frequency Ca^{2+} oscillations, i.e., whether it is a noise without any useful information, or a dynamic process, reflecting the physiological conditions (stimulation) in its temporal complexity, the latter has been found highly probable. The filtered Ca^{2+} series (Fig. 3, the top panel) has been tested against null hypotheses of white noise with the same histogram and of coloured noise with the same spectrum and histogram (using the so-called surrogate data approach¹⁶), which have been rejected with a high statistical significance. In other words, the considered noises, which mimic some properties of the filtered Ca^{2+} series, cannot produce such sharp changes in the CER values as observed in Fig. 3, the second panel from the top. Thus the segmentation of the series, obtained by the CER $h^{(0)}$, is due to stimulation-induced changes in the temporal complexity of the low amplitude high frequency Ca^{2+} dynamics.

6 Conclusion

It is well established that large amplitude low-frequency oscillations of $[\text{Ca}^{2+}]_i$ are an ubiquitous phenomenon in a number of electrically excitable and non-excitable cells^{1,2}. The interspike interval of these $[\text{Ca}^{2+}]_i$ spikes with amplitudes up to $1\mu\text{M}$ ranges between 30 sec and a couple of minutes. It has been demonstrated that the frequency and the amplitude of these repetitive $[\text{Ca}^{2+}]_i$ spikes can be modulated in a dose-dependent manner upon stimulation with an appropriate agonist. Although low amplitude fast $[\text{Ca}^{2+}]_i$ oscillations with $[\text{Ca}^{2+}]_i$ amplitudes in the range of 5 nM to 10 nM have been observed in experimental $[\text{Ca}^{2+}]_i$ time series under agonist stimulation, there has been no focus on characterizing the nature of these fast oscillations. The question if these fast oscillations carry any information beyond the information encoded

in the large amplitude low frequency $[\text{Ca}^{2+}]_i$ spikes has not been addressed yet. Our results indicate that the fast Ca^{2+} oscillations are nonlinear events since they are significantly different from isospectral linear stochastic processes. The deterministic nature of these oscillations is further supported since they are modulated by pharmacological stimulation. This has been demonstrated in the current study in clonal β -cells (HIT cells) using different doses of tolbutamide as stimuli. The coarse-grained entropy rates (CER's) which are computed from information-theoretic functionals - redundancies, are relative measures of regularity and predictability, and for data generated by dynamical systems they are related to the Kolmogorov-Sinai entropy. The CER's which have been demonstrated to be suitable for the classification of complex experimental time series in biological systems¹³ revealed considerable differences in the temporal dynamics of the fast Ca^{2+} oscillations in segments with and without stimulation by tolbutamide. Future studies of the functional relevance of these fast deterministic Ca^{2+} oscillations will have to demonstrate which semantic information they carry.

Acknowledgments

This work was supported by Deutsche Forschungsgemeinschaft under grant Scho 466/1-2 and Br 915/4-2. MP was supported by the Academy of Sciences of the Czech Republic.

Appendix - Estimation of the Marginal Redundancy

When the discrete variables X_1, \dots, X_n are obtained from continuous variables in a continuous probability space, then the redundancies $\varrho(X_1, \dots, X_{n-1}; X_n)$ depend on a partition ξ chosen to discretize the space. Various strategies have been proposed to define an optimal partition for estimating redundancies of continuous variables (see Refs. ^{11,12,16} and references therein). We have found that satisfactory results can be obtained by using simple box-counting method and by observing the following two rules:

- a) The partition is defined by the marginal equiquantization method, i.e., the marginal histogram bins are defined not equidistantly but so that there is approximately the same number of samples in each marginal bin.
- b) The relation between the number Q of quantization levels (marginal bins) and the effective^b series length N in the computation of n -dimensional redun-

^bIf a univariate series is used to construct a time-delay n -dimensional embedding (Eq. 4), the effective series length N is $N = N_0 - (n - 1)\tau$, where N_0 is the total series length, n is the embedding dimension, and τ is the time delay.

dancy should be

$$N \geq Q^{n+1},$$

otherwise the results may be heavily biased^{12,13}.

This algorithm does not provide unbiased estimates of absolute values, however, the absolute values of the redundancies are not important here. Applying this simple recipe and using the same parameters (N , n , Q and the τ -range), the redundancy estimator should bring consistent estimates in the relative sense that the marginal redundancies $\varrho^n(\tau)$ and, consequently, the CER's, obtained from different data/segments, are mutually comparable, and the CER's provide the classification of the data/segments equivalent to the classification given by the exact entropy rates¹³.

References

1. M.J. Berridge, *Nature* **361** 315 (1993).
2. D.E. Clapham, *Cell* **80** 259 (1995).
3. T.M. Cover and J.A. Thomas, *Elements of Information Theory* (J. Wiley & Sons, New York, 1991).
4. A.N. Kolmogorov, *Dokl.Akad.Nauk SSSR* **124** 754 (1959).
5. Ya.G. Sinai, *Dokl.Akad.Nauk SSSR* **124** 768 (1959).
6. I.P. Cornfeld, S.V. Fomin, Ya.G. Sinai, *Ergodic Theory* (Springer, New York, 1982).
7. K. Petersen, *Ergodic Theory* (Cambridge University Press, Cambridge, 1983).
8. Ya. G. Sinai, *Introduction to Ergodic Theory* (Princeton University Press, Princeton, 1976).
9. Ya.B. Pesin, *Russian Math. Surveys* **32** 55 (1977).
10. A.M. Fraser, *IEEE Transactions on Information Theory* **35** 245 (1989).
11. M. Paluš, in: *Time Series Prediction: Forecasting the Future and Understanding the Past*, (eds.) A.S. Weigend and N.A. Gershenfeld, Santa Fe Institute Studies in the Sciences of Complexity, Proc. Vol. XV (Addison-Wesley, Reading, Mass., 1993).
12. M. Paluš, *Neural Network World* **3/97** 269 (1997).
(<http://www.uivt.cas.cz/~mp/papers/rd1a.ps>)
13. M. Paluš, *Physica D* **93** 64 (1996).
14. J.D. Farmer, E. Ott and J.A. Yorke, *Physica D* **7** 153 (1983).
15. C. Schöfl *et al.*, *Endocrinology* **137** 3026 (1996).
16. M. Paluš, *Physica D* **80** 186 (1995).